Received: 2 November 2023 | Revised: 14 March 2024 | Accepted: 5 April 2024

DOI: 10.1002/ecs2.4875

ARTICLE

ECOSPHERE
AN ESA OPEN ACCESS JOURNAL

Few large or many small fires: Using spatial scaling of severe fire to quantify effects of fire-size distribution shifts

Michele S. Buonanduci[1,2] | **Daniel C. Donato**[2,3] | **Joshua S. Halofsky**[2,3] | **Maureen C. Kennedy**[4] | **Brian J. Harvey**[1,2]

[1]Quantitative Ecology and Resource Management, University of Washington, Seattle, Washington, USA

[2]School of Environmental and Forest Sciences, University of Washington, Seattle, Washington, USA

[3]Washington State Department of Natural Resources, Olympia, Washington, USA

[4]School of Interdisciplinary Arts and Sciences, University of Washington (Tacoma), Tacoma, Washington, USA

Correspondence
Michele S. Buonanduci
Email: mbuon@uw.edu

Funding information
Joint Fire Science Program, Grant/Award Number: Graduate Research Innovation Award #21-1-01-26; USGS Northwest Climate Adaptation Science Center, Grant/Award Number: G17AC000218

Handling Editor: Franco Biondi

Abstract

As wildfire activity increases and fire-size distributions potentially shift in many forested regions worldwide, anticipating the spatial patterns of burn severity expected with future fire activity is critical for ecological understanding and informing management and policy. Because spatial patterns of burn severity are influenced by a complex mixture of drivers, they remain difficult to predict for any given burned landscape. At broader extents, however, spatial scaling relationships relating high-severity patch size and shape to overall fire size, when combined with scenarios regarding regional area burned and fire-size distributions, offer a means to anticipate the spatial configuration of burn severity in future fires. Here, leveraging a satellite burn-severity dataset for 1615 fire events occurring across the northwest United States between 1985 and 2020, we present an approach for simulating expected patch-level burn-severity patterns at the scale of a region or fire regime of interest. We demonstrate this approach in a historically climate-limited fire regime within the Pacific Northwest, USA, where relatively infrequent but large and severe fires shape biomass-rich forests, and where fire potential is projected to increase as summer fire seasons become warmer and drier. We quantify how, for a given total burned area, the range of cumulative burn-severity patterns is expected to vary with the size distributions of fire events. Our results illustrate how shifts in fire-size distributions toward larger fire events will lead to increasingly large high-severity burn patches with interior areas that are increasingly far from unburned seed sources following fire. In contrast, the same total area burned in more numerous but smaller fire events will result in qualitatively different cumulative patterns of burn severity, characterized by smaller high-severity patches and closer proximity to postfire seed sources across burned landscapes. These results have important implications in forested regions, informing management actions ranging from prefire planning (e.g., fire response preparedness) to real-time decision-making (e.g., fire suppression vs. managed wildfire use) and postfire responses (e.g., replanting to

restore tree cover and/or promoting early-seral habitat). The approach we present is generalizable and can be applied across regions and fire regimes to anticipate potential future fire effects.

KEYWORDS
climate-limited fire regimes, fire ecology, fire-size distributions, future fire effects, high-severity burn patches, northwestern Cascadia, scaling relationships

INTRODUCTION

As climate warms worldwide, fire activity (i.e., area burned, fire frequency, and the occurrence of large fire events) is increasing in many forested ecosystems across the globe (Collins et al., 2021; Duane et al., 2021; Parks & Abatzoglou, 2020). Continued increases are projected for the next quarter-to-half-century in many regions (Littell et al., 2018), underscoring the importance of understanding both the nature and ecological consequences of changing fire regimes. While total area burned and fire size projections are important indicators of future fire activity and potential fire regime change, anticipating the ecological effects of wildfire requires also understanding the potential range of resulting burn-severity patterns. Management actions, both before and after the occurrence of fire (e.g., vegetation management and replanting), can promote climate-adapted landscapes and reduce negative postfire impacts on ecosystem services and forest function (Davis et al., 2023; Halofsky, Donato, et al., 2018b; Prichard et al., 2021). However, preemptively developing postfire response plans requires an understanding of the high-severity patch structure of individual fire events, as patches burned at high severity (i.e., areas in which most or all vegetation is killed by fire) are where postfire management intervention is often of greatest priority.

Of particular interest as fire potential increases in many fire-prone regions is understanding how, for a given total burned area, cumulative burn-severity patterns may differ depending on the size distribution of individual fire events (e.g., if the same total burned area is distributed as a few large fires vs. many smaller fires). In many fire-prone regions across the globe, fire-size distributions are "heavy-tailed"; in other words, most fire events are relatively small, yet most burned area comes from a few very large fire events (Agee, 1998; Hantson et al., 2016; Malamud et al., 2005; McKenzie & Kennedy, 2011). In the western United States, increasing temperature and aridity have been linked to increases in large, extreme fire spread events in recent decades (Juang et al., 2022), and shifts in fire-size distributions toward larger events are expected in many regions across North America with continued warming and drying climate (Coop et al., 2022; Wang et al., 2020). Beyond their substantial contributions to total burned area, the largest fire events tend to have the greatest cumulative ecological effects on forest structure (Cova et al., 2023; Romme et al., 2011). Thus, as fire-size distributions shift, a key question arises: How will fire-induced changes in forest structure (i.e., via large patches of severe fire with long distances to surviving trees) differ if an area is burned in few very large fires, compared with that same total area burning solely in small-to-moderate fire events? Understanding the cumulative ecological effects expected from varying fire-size distributions will be critical for fire management planning that seeks to maintain forest resilience.

The objective of this study was to quantify the potential cumulative burn-severity patterns (and therefore ecological effects) expected from differing fire-size distributions at a regional scale. Because spatial patterns of burn severity are influenced by a complex mixture of drivers, they can be difficult to predict for any given landscape (Newman et al., 2019; Parks, Holsinger, Panunto, et al., 2018a; Prichard et al., 2020). More broadly, however, high-severity patch structure is strongly related to fire size and exhibits characteristic spatial scaling relationships (i.e., as fire size increases, so does the potential for large high-severity patches within which burned areas are very far from unburned seed sources; Cansler & McKenzie, 2014; Collins et al., 2017; Harvey et al., 2016b). In the northwestern United States, the burn-severity patterns of wildfires occurring in recent decades (1985–2020) exhibit scaling relationships that vary by fire regime (i.e., infrequent, high-severity fire regimes vs. frequent, low-severity fire regimes) but appear otherwise stationary in both space and time (Buonanduci et al., 2023). Thus, when combined with projections for total area burned and fire-size distributions at regional scales, the consistency in these spatial scaling relationships can be harnessed to anticipate future fire effects.

To address this objective, we leverage a satellite-derived burn-severity dataset of 1615 fire events occurring across the northwestern United States between

1985 and 2020. We present an approach that uses spatial scaling relationships exhibited by contemporary wildfires to characterize the range of future burn-severity patterns that might be expected within a region or fire regime of interest. We ask: How might the range of potential burn-severity patch structure vary, depending on the size distribution of future fire events? Using simple fire-size distribution scenarios and a simulation-based approach, we assess how the cumulative effects of a given total burned area might vary, depending on whether the area burns in a small number of very large fires versus more numerous but smaller fire events.

The approach we present is generalizable across fire regimes and ecoregions, and as we show here, it can be used even in data-sparse regions with limited fire activity in the empirical record. As climate and fire activity continue to change, some of the largest future increases in area burned are expected to occur in historically cool, wet regions where fire activity has been limited by climate and ignitions rather than fuel (Littell et al., 2018; McColl-Gausden et al., 2022; Westerling et al., 2011). Climate-limited fire regimes are typically characterized by infrequent fires, with stand-level fire return intervals commonly on the order of centuries. Such regions therefore tend to be data-sparse in the observational record due to their limited fire activity. This paucity of empirical data limits the understanding of fire and fire effects and presents challenges for quantifying statistically robust scaling relationships (i.e., relationships between fire size and burn-severity patch metrics) using data solely from such regions. Fortunately, the consistency of scaling relationships observed within fire regimes across the northwestern United States (Buonanduci et al., 2023) suggests that the sparse empirical records of infrequent fire regions could be supplemented with data from comparable fire regimes, thus offering a means to quantify potential future burn-severity patterns in such regions. As an illustrative example, we demonstrate this approach using an archetypical infrequent fire region in the northwestern United States, the region west of the Cascade Crest in Washington and northern Oregon (hereafter "northwestern Cascadia"; Figure 1). Climate projections for northwestern Cascadia suggest summer fire seasons will become warmer and drier (Dalton et al., 2013; Mauger et al., 2015), and therefore the potential for fire activity, including very large fire events, is expected to increase (Halofsky et al., 2020; Halofsky, Conklin, et al., 2018a).

METHODS

Study region

Our study includes burn-severity data from the forested ecoregions of the northwestern United States (Wyoming, Montana, Idaho, Washington, Oregon, and northern

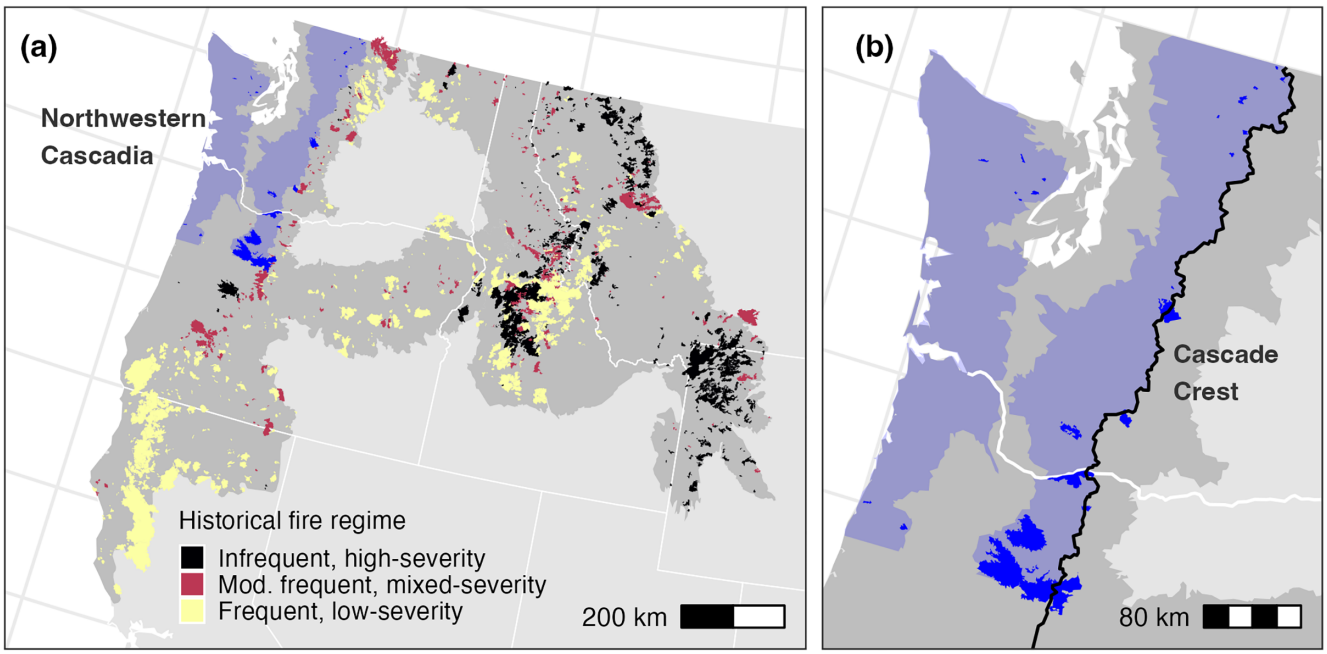

FIGURE 1 (a) Northwestern United States study area (dark gray) with fire events categorized by historical fire regime based on the most prevalent LANDFIRE fire regime group (frequent and low severity, moderately frequent and mixed severity, or infrequent and high severity) within each fire's perimeter. (b) Inset showing northwestern Cascadia region (light blue) and fire events (dark blue). Patch metrics for all northwestern Cascadia fire events were calculated only for the portion of each fire that burned west of Cascade Crest.

California), delineated using EPA Level III Ecoregions (Commission for Environmental Cooperation, 1997) (Figure 1). Climate, topography, and forest types vary widely across the northwestern United States (Hood et al., 2021; Reilly et al., 2021). Historical fire regimes range from frequent and predominantly low-severity fire in warmer and drier parts of the region to infrequent and predominantly high-severity fire in cooler and wetter parts of the region (Agee, 1993; Baker, 2009; Hood et al., 2021; Reilly et al., 2021).

Within the northwestern United States, the focal region that we use for our illustrative example is northwestern Cascadia (USA), the 6.1 million-ha forested region west of the Cascade Crest in Washington and northern Oregon (Figure 1). This region has a Mediterranean climate, with most precipitation falling during the winter (i.e., between October and April) and summers that are typically warm and dry (Donato et al., 2020; Reilly et al., 2022). Northwestern Cascadia is dominated by the high-elevation, topographically complex Olympic Mountains, Western Cascades, and Coast Range. The Puget Lowlands and Willamette Valley, which transect this region and are characterized by lower elevations and simpler topography, are not considered part of our study scope (Figure 1).

Forests in northwestern Cascadia are some of the most productive, biomass-rich ecosystems in the world (Donato et al., 2020; Reilly et al., 2021; Spies et al., 2018; Waring & Franklin, 1979). The primary vegetation zone in northwestern Cascadia is the moist Douglas-fir/western hemlock zone, dominated by Douglas-fir (*Pseudotsuga menziesii*) successional to western hemlock (*Tsuga heterophylla*), with Pacific silver fir (*Abies amabilis*) and mountain hemlock (*Tsuga mertensiana*) vegetation zones occurring at the highest elevations (Reilly et al., 2021). These forests have historically been characterized by long intervals (i.e., >150 years) between large and severe wildfires (Agee, 1993; Hemstrom & Franklin, 1982; Reilly et al., 2021), with non-stand-replacing fire events also occurring between large fire events (Tepley et al., 2013). Due to the infrequent nature of wildfire in this region, few wildfires ($n = 31$) have occurred in northwestern Cascadia since the beginning of the Landsat satellite record (1985–2020). Though infrequent, large fire events in northwestern Cascadia have historically burned extensive areas (i.e., 10^5–10^6 ha), with the largest fire events typically occurring when prolonged summer drought, an ignition, and a strong, synoptic east wind event coincide (Donato et al., 2020; Reilly et al., 2021). This was the case for the 2020 "Labor Day" fires in western Washington and Oregon, which collectively burned >300,000 ha over the course of just two weeks in September (Reilly et al., 2022). The southern boundary for northwestern Cascadia is drawn at 44°44′ N (ca. 20 km south of Salem, OR), as mixed- and low-severity fire regimes become more common at lower latitudes in western Oregon.

Burn-severity data

We used a satellite-derived burn-severity dataset first described by Buonanduci et al. (2023), consisting of all fire events ≥400 ha in size occurring within the northwestern United States between 1985 and 2020. Fire perimeters were obtained from the Monitoring Trends in Burn Severity database (https://mtbs.gov/), with prescribed fires and fire events occurring in primarily nonforest areas (<50% forested based on LANDFIRE Environmental Site Potential [ESP]) excluded (Rollins, 2009). Fire events were designated northwestern Cascadia fires if they intersected the northwestern Cascadia region and burned ≥400 ha west of the Cascade Crest. Each fire event falling outside of northwestern Cascadia was classified into one of three historical fire regimes based on the most prevalent LANDFIRE fire regime group (FRG) mapped within that fire's perimeter (Figure 1): frequent and predominantly low-severity fire (FRG I), moderately frequent and mixed-severity fire (FRG III), or infrequent and predominantly high-severity fire (FRG IV and FRG V; Rollins, 2009). In total, our dataset consisted of 1615 individual fire events, with 31 northwestern Cascadia fires and 751, 361, and 472 northwestern United States fires assigned to the frequent/low-severity, moderately frequent/mixed-severity, and infrequent/high-severity FRGs, respectively.

Burn-severity maps were generated for each fire event using 30-m resolution Landsat satellite data, following methods outlined by Parks, Holsinger, Voss, et al. (2018b). To quantify burn severity, we used the relativized differenced normalized burn ratio (RdNBR), a metric that compares prefire and postfire indices corresponding to vegetation and fire-caused change (Miller & Thode, 2007). Our calculation of RdNBR included an offset term to account for phenological differences between pre- and postfire imagery and to facilitate comparison of RdNBR between fire events (Parks, Holsinger, Voss, et al., 2018b). Following Harvey et al. (2023), we used statistical models calibrated to northwestern United States field plots (Saberi & Harvey, 2023) to identify a threshold of RdNBR (RdNBR ≥ 542) corresponding to ≥75% tree basal area mortality. We then used this threshold to categorize each burn-severity map into high (RdNBR ≥ 542) and low-to-moderate (RdNBR < 542) burn-severity classes. Satellite index thresholds have been shown to provide reliable approximations of high-severity burned areas

(Lydersen et al., 2016) and have been used in many regional-scale burn-severity studies (Parks, Holsinger, Panunto, et al., 2018a; Reilly et al., 2017; Singleton et al., 2019; Stevens et al., 2017).

Landscape metrics

We quantified high-severity patch size and structure using landscape metrics described by Buonanduci et al. (2023). First, we delineated high-severity patches using an eight-neighbor rule after applying a majority smoothing filter to each categorized burn-severity map. Second, for pixels within each high-severity patch that were potentially forested (based on LANDFIRE ESP) prior to burning, we quantified the distance to seed source by calculating the distance to the nearest potentially forested pixel that did not burn at high severity. Finally, we calculated five landscape metrics for each fire event (Table 1), with landscape metrics for northwestern Cascadia fires calculated using only the portion of each fire that burned west of the Cascade Crest.

We quantified the size distribution of high-severity patches within each fire event using two approaches (Table 1). First, we calculated the area-weighted mean patch size. Second, following the approach proposed by Buonanduci et al. (2023), we fit a truncated lognormal probability density function (Hantson et al., 2016) characterized by two shape parameters (β and ψ) to each patch-size distribution. The probability density function, $p(x)$, takes the following form:

$$\ln p(x) = \ln C - \beta \ln(x) - \psi[\ln(x)]^2, \quad (1)$$

where C is a normalization constant, ensuring the area under $p(x)$ sums to 1. Within the lower and upper truncation limits (set equal to 1 ha and the size of each fire event, respectively), the parameters β and ψ determine the shape of each probability distribution. Fitted values of β and ψ are highly correlated, with β strongly decreasing as ψ increases (Buonanduci et al., 2023; Hantson et al., 2016). When ψ is equal to 0, the distribution reduces to a power law function, and the shape of the distribution is a straight line in log–log space, with β determining the slope. When ψ is negative, patch-size distributions curve upward in log–log space and are typically characterized by one or more very large patches. When ψ is positive, patch-size distributions curve downward in log–log space and are typically characterized by many small patches.

We also quantified the structure of high-severity patches within each fire event using two approaches (Table 1). First, we calculated the total core area, which includes all previously forested pixels within the interior of high-severity patches that are >150 m from potential seed source following fire. The 150-m distance-to-seed

TABLE 1 Description of landscape metrics for high-severity patches used in the analysis.

Metric	Units	Description
Patch size metrics		
Area-weighted mean patch size	ha	The expected patch size that would be encountered at an average location within the burned landscape (Harvey et al., 2016b).
β and ψ	unitless	Parameters characterizing the shape of each patch-size frequency distribution. When ψ is equal to 0, the distribution resembles a power law function, and the shape of the distribution is a straight line in log–log space. When ψ is negative, patch-size distributions curve upward in log–log space and are typically dominated by one or more very large patches. When ψ is positive, patch-size distributions curve downward in log–log space and are typically characterized by many small patches (Buonanduci et al., 2023; Hantson et al., 2016).
Patch structure metrics		
Total core area	ha	Sum of all forested areas within the interior of high-severity patches that are >150 m from potential seed source following fire. This distance-to-seed threshold exceeds the likely seed dispersal distance for many conifer species in the northwestern United States (Greene & Johnson, 1989; Harvey et al., 2016a; Kemp et al., 2016).
Stand-replacing decay coefficient (SDC)	unitless	Parameter characterizing the rate at which the interior forested area of high-severity patches shrinks with an increasing distance-to-seed threshold. Larger values indicate a rapidly decaying interior area (i.e., most forested areas that burned at high severity are relatively close to potential seed sources), whereas smaller values indicate a more slowly decaying interior area (i.e., more forested areas that burned at high severity are far from potential seed sources) (Collins et al., 2017).

threshold exceeds the likely seed dispersal distance for many wind-dispersed conifers in the northwestern United States (Greene & Johnson, 1989; Harvey et al., 2016a; Kemp et al., 2016). Second, we fit a parameter (the stand-replacing decay coefficient [SDC]) characterizing the rate at which the forested area within the interior of high-severity patches shrinks with increasing distance to potential seed source. Following the approach proposed by Collins et al. (2017), we used a modified logistic function to model the proportion of total high-severity or "stand-replacing" forested area, P_{dts}, exceeding a given distance to potential seed, dts, as follows:

$$P_{\text{dts}} \sim \frac{1}{10^{\text{SDC} \times \text{dts}}}. \quad (2)$$

Larger values of the SDC parameter indicate a rapidly decaying interior area, whereas smaller values of SDC indicate a more slowly decaying interior area (Collins et al., 2017).

We calculated area-weighted mean patch size and total core area using the sf and raster packages in R (Hijmans et al., 2022; Pebesma, 2018). For each fire event with ≥10 patches exceeding 1 ha in size, we fit patch-size distribution shape parameters (β and ψ) using the maximum likelihood algorithm proposed by Pueyo (2014). Finally, we summarized inverse cumulative distance-to-seed distributions for each fire event using 30-m bins of pixel-level distance-to-seed and fit SDC parameters using nonlinear least squares, following Collins et al. (2017).

Scaling relationships

Following the approach used by Buonanduci et al. (2023), we used nonparametric quantile regression to quantify spatial scaling relationships. Rather than estimating the conditional mean of a response variable distribution, quantile regression estimates the conditional quantiles, providing a fuller picture of the response distribution (Cade & Noon, 2003; Koenker & Bassett, 1978). Within each northwestern United States FRG (frequent/low severity, moderately frequent/mixed severity, infrequent/high severity), we fit smooth curves to multiple conditional quantiles of each patch metric across the range of observed fire sizes. We constrained quantile curves to be monotonically increasing for area-weighted mean patch size and total core area and monotonically decreasing for the distance-to-seed parameter (SDC). No monotonicity constraints were imposed for the patch-size distribution parameters (β and ψ). Area-weighted mean patch size, total core area, and SDC were $\log_{10}$-transformed prior to model fitting, and in cases where total core area was zero, we added 0.01 ha to enable $\log_{10}$-transformation. All quantile curves were fit via additive basis splines using the quantregGrowth package in R (Muggeo, 2021).

After quantifying fire-regime-specific scaling relationships, we compared northwestern Cascadia with the three broad FRGs in the northwestern United States and determined that high-severity patch metrics in northwestern Cascadia exhibited scaling behavior comparable to other infrequent, high-severity fire regimes in this broader region (Figure 2; Appendix S1). Given the relative paucity of data for northwestern Cascadia ($n = 31$ wildfires) and the consistency observed between northwestern Cascadia and the broader northwestern United States infrequent/high-severity FRG (Figure 2), we decided to pool the sparse data for northwestern Cascadia together with the data from this comparable fire regime. After supplementing the northwestern Cascadia data in this way, we fit quantile regression models to the pooled dataset for each spatial metric, and these scaling relationships formed the basis of the simulation study described below.

Simulation study

To quantify how the future range of burn-severity patch structure might vary depending on the sizes of future fire events, we implemented a simulation study (Figure 3) that harnessed the range of variation in spatial scaling relationships expected for our focal region. Using northwestern Cascadia as our illustrative example, we asked: Assuming a total area of 1,000,000 ha were to burn, what would the potential range of ecological effects be if this area were to burn as (A) 10 very large fires (each 100,000 ha), (B) 100 moderately large fires (each 10,000 ha), or (C) 1000 smaller fires (each 1000 ha)? A total burned area of 1,000,000 ha would constitute 16% of the northwestern Cascadia region and corresponds with the upper end of size estimates for historical fire episodes in this region (Donato et al., 2020). As a simple case study, we considered hypothetical fire sizes spanning three orders of magnitude (1000–100,000 ha) (Figure 3a). For context, recent notable fire events in northwestern Cascadia have spanned these same three orders of magnitude (e.g., the 2015 Paradise fire in Washington [1140 ha], the 2020 big Hollow fire in Washington [9811 ha], and the 2020 Beachie Creek fire in Oregon [78,761 ha]).

To conduct this simulation study, we used the spatial scaling relationships for northwestern Cascadia (in the form of quantile regression models; see previous

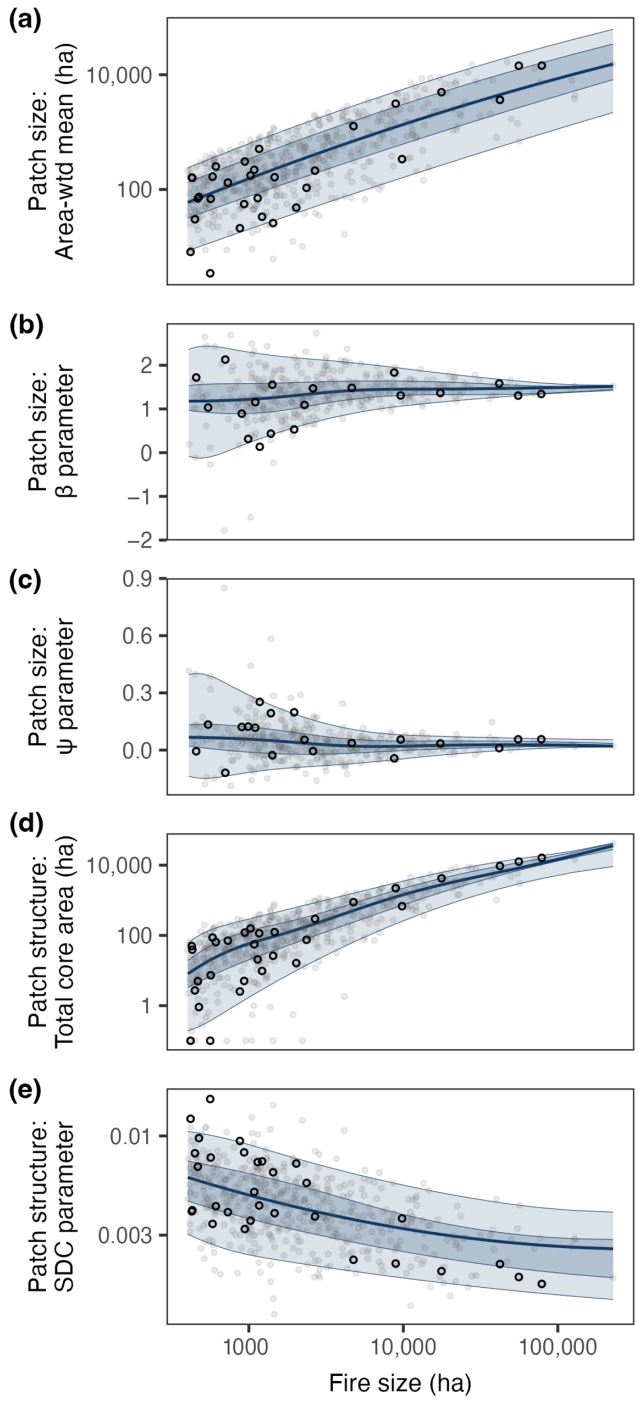

FIGURE 2 Northwestern Cascadia patch metrics (black open circles) overlaid on patch metrics from fires occurring within other infrequent, high-severity regimes in the northwestern United States (gray dots). Lines and shading represent scaling relationships quantified for the pooled dataset; solid line is quantile 0.5, dark shaded region is the interval between quantiles 0.25 and 0.75, and light shaded region is the interval between quantiles 0.05 and 0.95. SDC, stand-replacing decay coefficient; wtd, weighted.

section and Figure 2) to simulate a core area, distance-to-seed distribution, and patch-size distribution for each hypothetical fire event based on its size (simulation workflow described in Figure 3b–d and below). We aggregated the simulated metrics across fire events in each scenario (e.g., for total core area in Scenario A, we summed together the individual core areas simulated for each of the 10 hypothetical fires) to quantify cumulative effects across the hypothetical 1,000,000 ha burned. Each scenario was simulated 100 times. Following Kennedy (2019), who used principles of experimental design to determine the number of replicates necessary to detect a given effect size for a stochastic model, we determined 100 replicates would be sufficient to detect aggregate core area effect sizes up to 9000 ha.

The number of steps required to simulate each spatial metric varied, with total core area being the most straightforward, as it is an aggregate metric for each fire in units (hectares) that can simply be summed across fire events. To simulate the total core area (Figure 3b), we fit smooth curves to 99 conditional quantiles (0.01 through 0.99) of the total core area distribution across the range of observed fire sizes. Then, to simulate the total core area for a fire of any given size, we extracted the 99 conditional quantile predictions at that fire size and randomly drew one value. This sampling approach is a coarse and empirical adaptation of inverse transform sampling, a method that is frequently used to generate random samples from known probability distributions (Devroye, 1986). In our analysis, we defined core area using a 150-m distance-to-seed threshold; however, the distance at which tree regeneration becomes limited varies by region and dominant tree species. Therefore, to evaluate the sensitivity of our findings to the distance-to-seed threshold used to define core area, we replicated our simulation study for core areas calculated using a 300-m distance threshold.

For the distance-to-seed and patch-size distributions, additional assumptions and simulation steps were required. From the SDC parameter, we can calculate (using Equation 2) a proportional distance-to-seed distribution for each fire event. Aggregating distance-to-seed distributions across fire events, however, requires calculating each distance-to-seed distribution in terms of areas (i.e., in hectares); doing so requires knowing the total area within each fire that was both forested and burned at high severity. Similarly, from the β and ψ parameters, we can randomly draw (using Equation 1) some number of patch sizes for each fire event from a truncated lognormal distribution. Aggregating patch-size distributions across fire events, however, requires constraining the random sample of high-severity patches drawn for each fire, such that the total area of all high-severity patches is equal to the total high-severity burned area for that fire. Thus, for the distance-to-seed distributions, we needed to

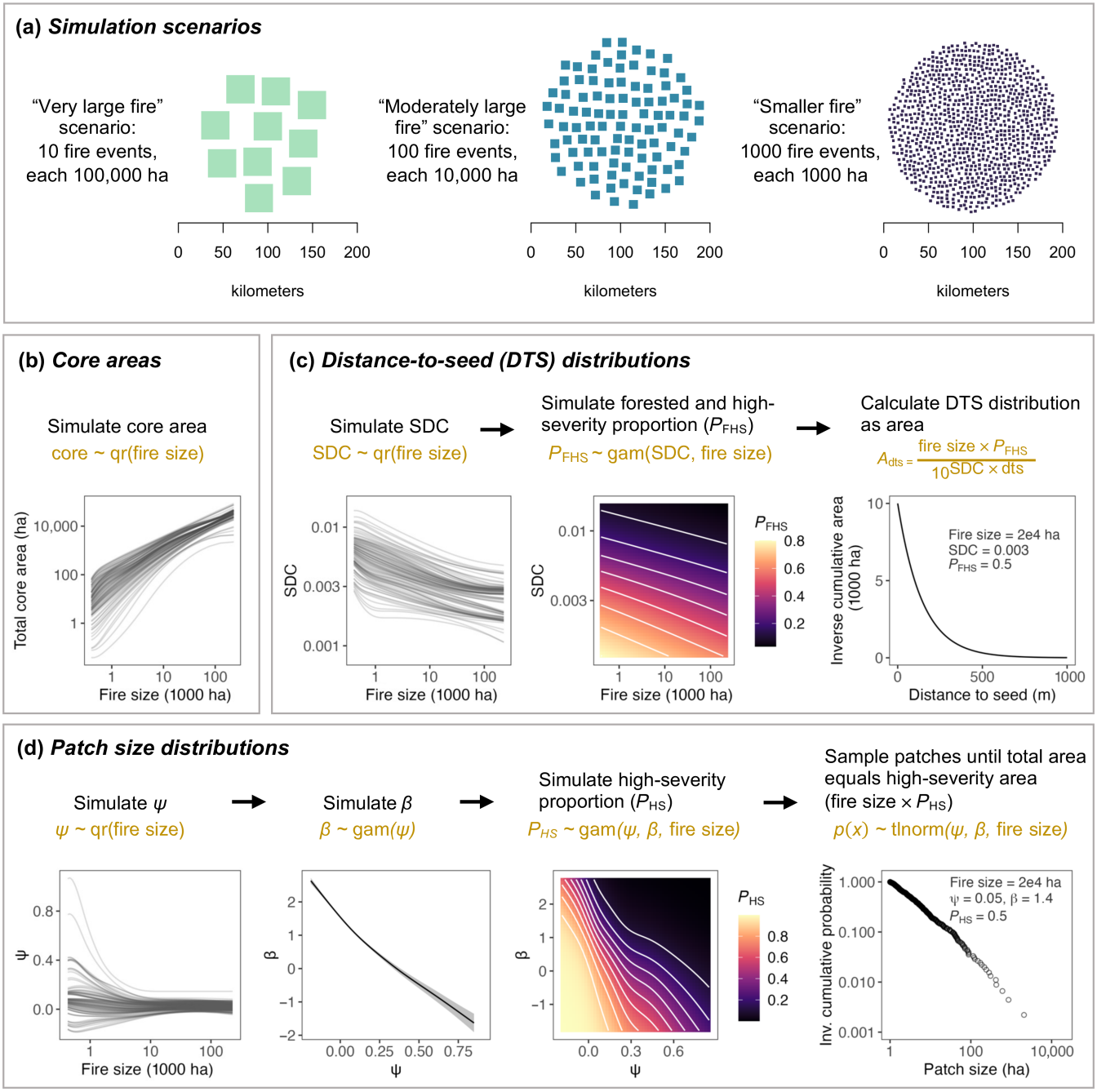

FIGURE 3 (a) Conceptual illustration of simulation scenarios, along with schematics of simulation study workflows for (b) core areas based on a 150-m seed distance, (c) distance-to-seed (DTS) distributions, and (d) patch-size distributions. For more detailed information regarding simulation study methods, see Appendix S2. gam, generalized additive model; qr, quantile regression; tlnorm, truncated lognormal; SDC, stand-replacing decay coefficient.

simulate the forested and high-severity proportion (P_{FHS}) of each fire (in addition to simulating SDC), and for the patch-size distributions, we needed to simulate the high-severity proportion (P_{HS}) of each fire (in addition to simulating β and ψ).

Across fire events, landscape metrics describing spatial patterns of burn severity naturally tend to be correlated with one another (Neel et al., 2004). In our dataset, we observed that fire size, SDC, and P_{FHS} were correlated with one another, as were fire size, β, ψ, and P_{HS}. This correlation enabled us to sequentially simulate sets of parameters jointly falling within the range of variation observed in our dataset. For example, once fire size is fixed, the conditional range of variation in SDC is reduced and we can sample from its conditional distribution given fire size; then, once fire size and SDC are

fixed, the conditional range of variation in P_{FHS} is reduced and we can sample from its conditional distribution given fire size and SDC. We followed this logic for the simulation of both distance-to-seed and patch-size distributions, as described below.

To simulate distance-to-seed distributions (Figure 3c), we first fixed fire size and simulated a value for SDC using the quantile regression approach described above for the total core area. After simulating the SDC parameter, we simulated P_{FHS} for each fire using a generalized additive model (GAM) fit to P_{FHS} as a function of SDC and fire size. Finally, we used the simulated SDC parameter to calculate an area-based distance-to-seed distribution, where the cumulative area (in hectares) exceeding each distance-to-seed threshold (A_{dts}) is calculated as a function of fire size, P_{FHS}, and SDC as follows:

$$A_{dts} = \frac{\text{fire size} \times P_{FHS}}{10^{SDC \times dts}}. \quad (3)$$

Equation (3) is a modified version of Equation (2), where fire size and P_{FHS} are included as additional parameters to calculate an area-based rather than a proportional distance-to-seed distribution.

To simulate patch-size distributions (Figure 3d), we first fixed fire size and simulated a value for ψ using the quantile regression approach described above for total core area and SDC. We then simulated a value for β, which is highly correlated with ψ, using a GAM fit to β as a function of ψ. After simulating the ψ and β parameters, we simulated P_{HS} for each fire using a GAM fit to P_{HS} as a function of ψ, β, and fire size. Finally, we used the simulated ψ and β to parameterize a truncated log-normal distribution, from which we sampled patches until the total area of patches equaled the simulated high-severity area (A_{HS}; calculated as fire size multiplied by P_{HS}). GAMs were fit using the mgcv package in R (Wood, 2022). For a more detailed description and additional information regarding simulation study methods, see Appendix S2.

RESULTS

Across simulation scenarios, as the sizes of fire events composing the hypothetical total 1,000,000 ha burned area increased (i.e., as burned area came from fewer but larger fire events), aggregate core areas increased and aggregate distance-to-seed distributions shifted to the right (i.e., greater amounts of forested area that burned at high severity were farther from potential live seed sources) (Table 2, Figure 4). Aggregate core area increased substantially between the smallest (i.e., 1000 ha) fire-size scenario (mean simulated core area = 88,775 ha, or 8.9% of the total burned area) and each of the larger fire-size scenarios, although it did not differ between the moderately large (i.e., 10,000 ha) and very large (i.e., 100,000 ha) fire-size scenarios (mean simulated core areas = 154,720 and

TABLE 2 Descriptive statistics for simulated aggregate core areas and distance-to-seed distributions, summarized over 100 iterations of each simulation scenario.

		Area exceeding distance-to-seed threshold (ha)			
Distance-to-seed threshold	**No. and size of fire events**	**Mean**	**SD**	**Min**	**Max**
Core area approach					
150 m	10 × 100,000 ha	154,557	18,489	113,390	198,879
	100 × 10,000 ha	154,720	10,848	126,371	181,922
	1000 × 1000 ha	88,775	2991	83,359	97,209
Distance-to-seed distribution approach					
150 m	10 × 100,000 ha	187,575	31,002	116,662	255,201
	100 × 10,000 ha	148,436	7965	131,418	167,847
	1000 × 1000 ha	90,899	2525	84,308	97,320
450 m	10 × 100,000 ha	41,786	12,529	17,075	74,860
	100 × 10,000 ha	22,734	2323	17,867	28,281
	1000 × 1000 ha	8967	522	7735	10,053
750 m	10 × 100,000 ha	10,770	4524	2409	24,702
	100 × 10,000 ha	4311	622	3124	6065
	1000 × 1000 ha	1325	123	1048	1580

Abbreviations: Max, maximum; min, minimum.

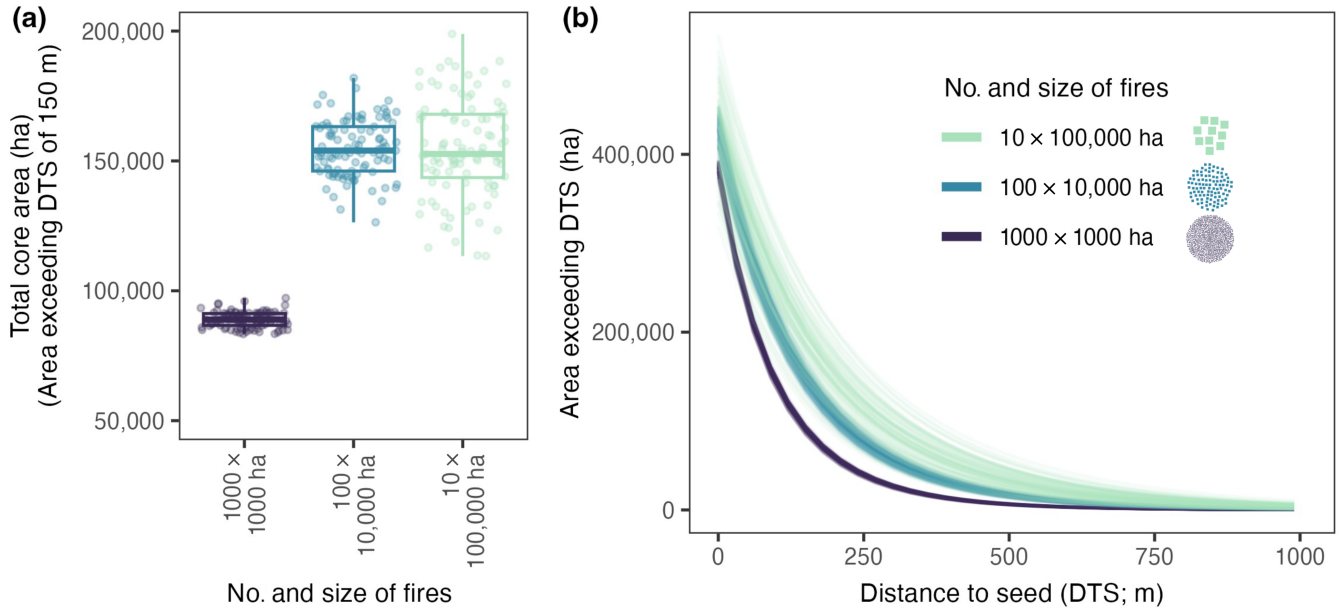

FIGURE 4 Simulated aggregate (a) core areas based on a 150-m seed distance and (b) continuous distance-to-seed (DTS) distributions. Each scenario represents the same hypothetical total area burned (1,000,000 ha) and was simulated 100 times, with each iteration displayed as a single data point in (a) and a single line in (b).

154,557 ha, respectively, or 15.5% of the total burned area; $p > 0.05$ using ANOVA and Tukey's honestly significant difference [HSD] test) (Table 2, Figure 4a). This potential asymptote in aggregate core area with increasing fire size (i.e., lack of difference between the moderately large and very large fire-size scenarios) was sensitive to the distance-to-seed threshold used to define core area. When we increased the distance threshold from 150 to 300 m, aggregate core area consistently increased across fire-size scenarios, with mean simulated core areas of 18,808, 57,547, and 72,842 ha (1.9%, 5.8%, and 7.3% of the total burned area) for the small, moderately large, and very large fire-size scenarios, respectively (Appendix S2).

As fire sizes increased, the tails of the aggregate distance-to-seed distributions became heavier (i.e., more high-severity burned area exceeded greater distance-to-seed thresholds). For example, aggregate areas exceeding a distance of 750 m to the nearest unburned seed source were 1325, 4311, and 10,770 ha (0.1%, 0.4%, and 1.1% of the total burned area) on average in the small, moderately large, and very large fire-size scenarios, respectively (Table 2, Figure 4b). Area estimates in the tails of the simulated distance-to-seed distributions are likely to be overestimates, as actual patch interior areas will reach zero with increasing distance-to-seed, whereas the modified logistic function we used to model distance-to-seed distributions (Equations 2 and 3) only approaches zero (Collins et al., 2017). Nevertheless, the simulated distributions (Figure 4b) provide reasonable approximations of the effect of increasing fire size.

By definition, aggregate core area estimates in our study represent the total forested area burned at high severity and exceeding a threshold of 150 m to seed, and thus can be directly compared to aggregate distance-to-seed distribution estimates at that same threshold. The two approaches yielded qualitatively similar results, though estimates from the distance-to-seed distribution approach were biased slightly high relative to estimates from the core area approach in the very large fire-size scenario (Table 2, Appendix S2).

Simulated aggregate patch-size distributions were characterized by increasingly large patches as the sizes of fire events increased (Table 3, Figure 5). Area-weighted mean patch sizes consistently increased with the size of fire events, as did maximum patch sizes, the latter of which ranged from 602 to 811 ha across iterations in the smallest fire-size scenario, from 5406 to 8166 ha across iterations in the moderately large fire-size scenario, and from 19,419 to 68,172 ha across iterations in the very large fire-size scenario (Table 3, Figure 5). Most patches across fire-size scenarios were relatively small, with median patch sizes of ~3 ha on average across iterations and scenarios (Table 3). On average, in both the moderately large and very large fire-size scenarios, only 0.8% of simulated patches exceeded 1000 ha in size. Despite representing a small proportion in terms of the total number of patches, the contribution of large patches to the total high-severity burned area in these scenarios was substantial; on average, patches ≥1000 ha accounted for 48% of the total high-severity burned area in the

TABLE 3 Descriptive statistics for simulated aggregate patch-size distributions, summarized over 100 iterations of each simulation scenario.

	Median patch size (ha)				Area-weighted mean patch size (ha)				Maximum patch size (ha)			
No. and size of fire events	Mean	SD	Min	Max	Mean	SD	Min	Max	Mean	SD	Min	Max
10 × 100,000 ha	3.4	0.5	2.4	5.1	11,487	4208	4587	21,754	42,457	11,043	19,419	68,172
100 × 10,000 ha	3.3	0.1	3.0	3.6	1594	162	1194	2008	6658	569	5406	8166
1000 × 1000 ha	3.4	0.1	3.3	3.6	146	5	132	158	708	41	602	811

Abbreviations: Max, maximum; min, minimum.

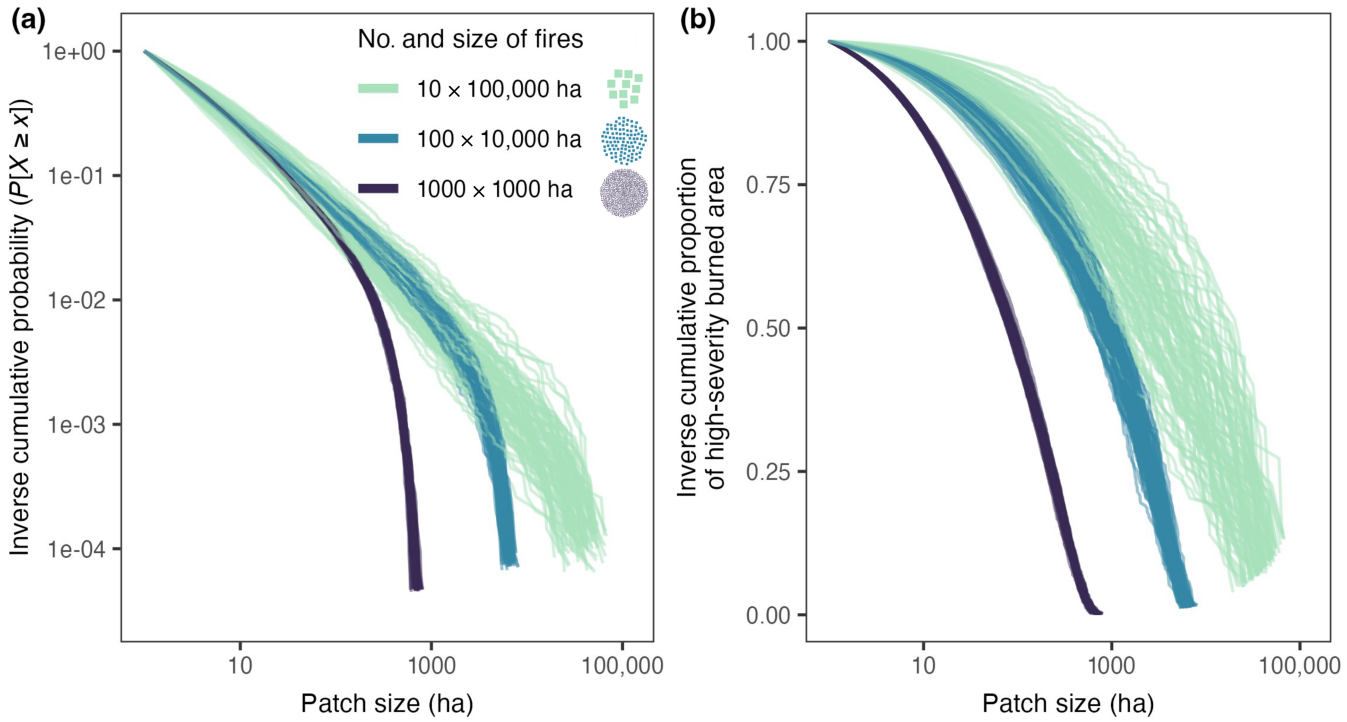

FIGURE 5 Simulated aggregate patch-size distributions, displayed as (a) inverse cumulative probability distributions and (b) inverse cumulative proportions of total high-severity burned area. Each scenario represents the same hypothetical total area burned (1,000,000 ha) and was simulated 100 times, with each iteration displayed as a single line. Note that the *y*-axis in (a) is log-transformed, but the *y*-axis in (b) is not.

moderately large fire-size scenario (ranging from 39% to 56%) and 66% of the total high-severity burned area in the very large fire-size scenario (ranging from 45% to 84%) (Figure 5b).

Finally, we observed that the variation in simulated aggregate metrics consistently increased across fire-size scenarios (Tables 2 and 3, Figures 4 and 5). For example, the SD of simulated aggregate core area increased by a factor of 4 between the small and moderately large fire-size scenario, and by a factor of 2 between the moderately large and very large fire-size scenarios (Table 2). This finding was even more pronounced for the simulated patch-size distributions; for example, the SD of maximum simulated patch sizes increased by a factor of 14 between the small and moderately large fire-size scenarios, and by a factor of 19 between the moderately large and very large fire-size scenarios (Table 3).

DISCUSSION

Our study demonstrates how burn-severity spatial scaling relationships can be used to simulate potential future ranges of cumulative burn-severity patterns, even in regions for which empirical fire data are lacking. The fire-size scenarios evaluated in our case study illustrate how for a given total burned area, near-term shifts in

fire-size distributions toward larger fire events will likely lead to increasingly large high-severity burn patches with interior areas that are increasingly far from unburned seed sources following fire. Conversely, the same total burned area occurring in more numerous but smaller fire events will likely result in burn-severity patterns characterized by smaller patches and greater proximity to unburned seed sources following a fire. We demonstrate this approach for northwestern Cascadia, a historically climate-limited region that is expected to see large increases in area burned with warming and drying climate. More broadly, however, our results have important forest and fire management implications across a range of fire regimes and ecoregions.

Shifts in fire-size distributions toward larger fire events will likely lead to larger and more homogeneous areas burned at high severity

By quantifying the range of burn-severity metrics expected across a range of potential fire sizes, we were able to simulate how the effects of a given total burned area might vary, depending on how it is distributed in terms of number and size of individual fire events. The simple scenarios used here bookend a range of potential future fire-size distributions. In regions where fire-size distributions are expected to shift to the right (i.e., increase in size) with changing climate (Coop et al., 2022; Wang et al., 2020), our findings illustrate how the size and spatial homogeneity of high-severity patches will also consistently increase, carrying implications for forest resilience in a period of increasing fire activity. In the western United States, increasing aridity in recent decades has been linked to both increasing annual area burned and increasing fire event sizes (Juang et al., 2022), and these trends are expected to continue in the near future (Parks & Abatzoglou, 2020). Even if the total area burned were to remain the same, as assumed in our simulation study, a shift toward larger fire events will likely result in larger high-severity patches with interior areas farther from live seed sources following fire. In forest ecosystems, the increasing size and homogeneity of high-severity patches will directly affect seed dispersal (Gill et al., 2022), rates of tree regeneration (Harvey et al., 2016a), formation and persistence of early-seral habitat (the stage between stand-replacing disturbance and tree canopy closure), and the potential for conversion to nonforest systems (Coop et al., 2020) following fire.

Our generalizable approach can be used to anticipate shifts toward either end of any fire-size distribution. For example, in our focal region of northwestern Cascadia, the scenarios ranged from the many small-fire scenario (1000 fire events, each 1000 ha in size) on one end to the few large fire scenario (10 fire events, each 100,000 ha in size) on the other. Climate projections for northwestern Cascadia suggest conditions conducive to fire will increase, with summer fire seasons projected to become warmer and drier (Dalton et al., 2013; Mauger et al., 2015). However, the largest fire events in northwestern Cascadia are typically driven by synoptic east wind events (Donato et al., 2020; Reilly et al., 2022), and it is still unclear whether and how the frequency of these events might shift moving forward. Therefore, reliable fire-size distribution projections (i.e., estimates of the relative frequency of small-to-moderate vs. very large fires) under a changing climate are not currently available for northwestern Cascadia. As more refined projections for annual burned area and fire-size distributions become available for this and other regions, the approach and scaling relationships presented here can be applied to such projections to provide more realistic estimates of future burn-severity patterns.

Our finding that aggregate core area did not differ between the two largest fire-size scenarios suggests that once fire-size distributions become sufficiently large (e.g., composed of individual fire events ≥10,000 ha), the total forested area burned at high severity and located >150 m from the nearest unburned seed source may begin to asymptote. Interestingly, this asymptotic behavior did not emerge when we increased the distance threshold used to define core area from 150 to 300 m (Appendix S2). In general, the longer the distance-to-seed threshold, the larger the high-severity patches required to produce interior areas exceeding said threshold, and the more strongly fire size itself constrains the occurrence of such patches. Our findings suggest 150-m core areas are strongly constrained by fire size in the smallest fire scenario (i.e., 1000 ha fires), but that once fires surpass the moderately large size threshold (i.e., 10,000 ha), fire size becomes less constraining and aggregate 150-m core areas level off. Conversely, 300-m core areas appear to be constrained by fire size in both the small and moderately large fire scenarios, as evidenced by the consistent increase in aggregate 300-m core areas across fire-size scenarios. Thus, while area exceeding a 150-m distance-to-seed threshold may asymptote as fire-size distributions shift to the right, areas exceeding longer distance-to-seed thresholds will likely continue to increase. This conclusion is supported by our continuous distance-to-seed distribution findings, which suggest that the tails of these distributions grow consistently heavier with increasing fire size. Increases in the tails of distance-to-seed distributions are expected to amplify postfire ecological effects, including slowing forest

recovery trajectories (Gill et al., 2022; Harvey et al., 2016a) and increasing persistence of early-seral habitats. The ecological relevance of specific distance-to-seed thresholds will vary by region and context, highlighting the importance of linking these findings to region-specific seed dispersal parameters.

Gaining insights for data-sparse and infrequent fire regions

Fire activity in many climate-limited fire regimes has been relatively rare since the beginning of the contemporary satellite record, presenting challenges for understanding and anticipating future fire effects. Yet, increasing fire activity is poised to profoundly shape such regions, which are often composed of biomass-rich forests that underpin ecosystem services region-wide. Our findings suggest that burn-severity patch structure scales consistently with fire size across infrequent, high-severity fire regimes in the northwestern United States. In light of this consistency, supplementing the empirical records of data-sparse regions with data from analogous fire regimes offers a means to quantify statistically robust scaling relationships, which can then be used to evaluate potential future fire effects. While this approach is especially useful in data-poor regions, it is generalizable and can also be applied to more frequent fire regions where empirical data are more readily available but the potential effects of future fire activity and changing fire regimes remain uncertain.

Implications for forest and fire management

Comparable burn-severity patterns can lead to varying forest regeneration trajectories and vegetation management considerations, depending on the fire-adapted traits of dominant tree species (Harvey et al., 2016a; Littlefield, 2019). In northwestern Cascadia, for example, most dominant tree species rely on dispersal of seeds from unburned live trees as the primary mechanism of tree regeneration following fire (Reilly et al., 2021). In general, postfire regeneration rates of conifer species that rely on wind-dispersed seeding will decrease with increasing distance to the nearest unburned seed source (Harvey et al., 2016a; Kemp et al., 2016; Littlefield, 2019). However, the distance at which tree regeneration becomes severely limited can vary widely; in northwestern Cascadia and other regions dominated by coastal Douglas-fir, robust postfire tree regeneration has been observed as far as 400 m from the nearest unburned seed source (Donato et al., 2009; Laughlin, 2023). Tree regeneration also varies with numerous additional factors, including prefire forest structure, topography, and postfire climate conditions (Davis et al., 2023; Laughlin, 2023; Littlefield, 2019). Therefore, planning for postfire replanting in locations predicted to exceed seed dispersal capacity will be important when maintaining forest cover is the management goal.

While large high-severity patches can be a concern for postfire forest recovery and resilience, they also underpin key aspects of ecosystem function by creating early-seral habitat (Halofsky, Donato, et al., 2018b; Steel et al., 2022). Naturally occurring early-seral forest ecosystems, including those that form following high-severity fire, are structurally complex and high in biodiversity, providing critical habitat for numerous plant and animal species (Swanson et al., 2011). Culturally important plant species, such as huckleberry (*Vaccinium myrtilloides* Michx.), thrive in such early-seral environments, and cultural fire has been used to promote habitat for these and other species for millennia (Johnston et al., 2023; LeCompte-Mastenbrook, 2015; Long et al., 2021; Wynecoop et al., 2019). Currently, structurally complex early-seral forest conditions are in a severe deficit in northwestern Cascadia, despite historically composing up to 30% of the landscape (Donato et al., 2020). While increasingly large high-severity patches will on the one hand slow tree regeneration rates, they will also in turn lead to an increasing persistence of early-seral habitat. As fire activity increases, therefore, the occurrence of large high-severity patches may help restore and maintain these ecologically and culturally important early-seral conditions (Halofsky, Conklin, et al., 2018a).

Our findings have important prefire and postfire management implications. First, when considering postfire replanting needs in northwestern Cascadia, we found that the amount of forest area burned at high-severity and located more than 150 m from an unburned seed source may asymptote around ~15% of the total burned area once fire-size distributions become sufficiently large (i.e., composed of individual fire events exceeding 10,000 ha). In other words, even in the largest fire-size scenarios, ~85% of total burned area is unlikely to require postfire replanting, being either burned at low-to-moderate severity and/or within the likely dispersal distance of unburned live seed sources. These proportions can provide a useful rule-of-thumb for managers planning for future fire events. Furthermore, given suitable postfire climate, it is possible for robust tree regeneration to naturally occur well beyond a distance of 150 m from unburned seed sources in northwestern Cascadia and similar regions dominated by tall trees such as coastal Douglas-fir (Donato et al., 2009; Laughlin, 2023);

therefore, these proportions provide likely upper-end estimates of the amount of area that may require postfire replanting. In areas where resources available for replanting may be limited and postfire tree cover is of management importance, efforts could focus on the largest high-severity patches where interior areas far exceed the likely dispersal distances of unburned seed sources. For example, our analysis suggests that <5% of total burned area is likely to be both burned at high severity and located more than 450 m from an unburned seed source following fire (ranging from 0.9% to 4.2% on average across fire-size scenarios). These are areas that may be in greatest need of postfire replanting, or alternatively, areas that may naturally be restored to early-seral habitat and likely to persist in this state following fire. While these proportions are modest, it is important to recognize that the areas may not be trivial, depending on the total area affected by fire.

Our findings also have real-time fire management implications, particularly in the decision-making realm regarding fire suppression versus managed wildfire use. In climate-limited fire regimes such as northwestern Cascadia, suppressing fires can in general be both an ecologically and socially defensible strategy (Halofsky, Donato, et al., 2018b), as fire suppression is necessary in many cases to protect human values and is unlikely to lead to the type of uncharacteristic fuel buildup that has occurred in historically fuel-limited regimes across the western United States (Hagmann et al., 2021). Managing forests for resilience to both fire and changing climate, however, could be enhanced by increasing species and structural diversity at a regional scale (Halofsky, Donato, et al., 2018b). Our results suggest that if all burned area in northwestern Cascadia came solely from relatively small (e.g., 1000 ha) fire events, fire activity would cumulatively have fine-grained effects on landscape patterns of forest structure. Conversely, the same total area burned in moderately large fire events (e.g., 10,000 ha) would have much coarser-grained effects, comparable in some ways to the cumulative effects of very large fire events (e.g., 100,000 ha). Therefore, allowing wildfires to reach a range of sizes (i.e., a practice of modified fire suppression) would meaningfully shape the heterogeneity and resilience of northwestern Cascadia forest landscapes by diversifying forest structure and successional pathways (Tepley et al., 2013). While managed wildfire use in this region has the potential to offer ecological benefits, it also presents socioeconomic risks, largely due to the potential for extreme weather (i.e., synoptic east winds) to develop, driving rapid fire growth and threatening human communities (Halofsky, Donato, et al., 2018b; Reilly et al., 2022). Given the high density of human populations and development in northwestern Cascadia, low-risk opportunities for managed wildfire use in this region may prove to be rare.

Model assumptions and limitations

Our modeling approach assumes that within each fire regime group, the relationships between fire size and patterns of burn severity (i.e., high-severity patch size and shape) are stationary in both space and time. In other words, after accounting for fire regime, we assume that the range of burn-severity patterns expected at any given fire size does not vary by region or time period. This assumption is well supported in the northwestern United States within contemporary fires observed in the satellite record (1985–2020; Buonanduci et al., 2023), despite this period being marked by increasing aridity, annual area burned, and fire event sizes (Juang et al., 2022). As fire activity continues to increase, however, fuel limitations may begin to strengthen in some regions, potentially altering fire size and severity through reductions in fuel availability and/or connectivity (Abatzoglou et al., 2021; Francis et al., 2023; Kennedy et al., 2021). It is possible that strengthening fuel limitations in such regions could also erode the stationarity in scaling relationships that has been observed over the contemporary record, with the range of high-severity patches shifting toward smaller sizes and more heterogeneous shapes at any given fire size. In northwestern Cascadia, however, where forests are highly productive and biomass-rich (Spies et al., 2018), fuel limitations are not likely to strongly constrain fires in the coming decades (Abatzoglou et al., 2021; Halofsky et al., 2020). Therefore, stationarity in scaling relationships is a reasonable assumption in northwestern Cascadia and many similar regions for the foreseeable future.

The only driver of burn-severity patterns that is explicitly accounted for in our modeling approach is fire size. By drawing from the full empirical distributions of patch size and shape across the range of observed fire sizes, we effectively integrate over a wide range of potential drivers, including vegetation types, fuel loads, weather at the time of burning, and fire management tactics. We feel that this approach is reasonable and appropriate, given the goal of modeling potential burn-severity patches over a large regional extent. In smaller landscapes or more specific contexts with a narrower range of possible drivers, however, our approach has the potential to over- or underestimate ecological effects. For example, it is possible that scaling relationships could differ between areas with greater or less fire management influence (e.g., wildland–urban interface vs. designated wilderness areas). Furthermore, there is historical precedence in northwestern Cascadia for areas burned in very large fires to partially reburn numerous times in the decades following the initial fire event (Reilly et al., 2022). When short-interval reburns such as these do occur, fuel limitations introduced by earlier fires can

limit high-severity patch size and homogeneity in subsequent fires. These types of negative feedbacks have mainly been observed in short-interval (e.g., <15 year) reburns in frequent, low-severity fire regimes of the northwestern United States, and less so in other fire regimes (Harvey et al., 2023). However, it is possible that our approach, which does not explicitly account for fuel loads, may not be appropriate for anticipating high-severity patch structure in landscapes burned multiple times within a few decades. Finally, ecological effects can be compounded in areas affected by short-interval reburns (Braziunas et al., 2023), particularly in areas that burn twice or more at high severity (Harvey et al., 2023; Turner et al., 2019). Modeling high-severity patch size and shape alone is not sufficient for anticipating potentially compound ecological effects that may occur in these contexts.

Our analysis is inherently limited by the observed fire size and severity data available within the contemporary satellite record. Given that fire-size distributions tend to be strongly right-skewed (McKenzie & Kennedy, 2011), the frequency of fire events and therefore the availability of empirical data naturally decreases as fire size increases. Because our approach relies on simulating from models fit to empirical distributions, the uncertainty in our model predictions and simulations therefore increases with fire size as the empirical data become increasingly sparse. This greater uncertainty, along with the wider range of variation in patch size and structure metrics that is observed for larger fire events, may partially explain the increasing variation in simulated patch metrics that we observed across fire-size scenarios. However, the increasing variation also arises in part from the simulation study design itself and the properties of the central limit theorem; because the number of simulated fires decreases across scenarios (i.e., 1000 fires are simulated in each iteration of the smallest fire-size scenario, compared with 100 fires in the moderately large fire-size scenario and 10 fires in the very large fire-size scenario), the variance in the sampling distribution naturally increases across scenarios. The increasing variation in simulated metrics across fire-size scenarios likely stems from both of these causes, though it is difficult in our approach to disentangle the two.

CONCLUSION

Anticipating the ecological effects of future fire activity is broadly challenging, particularly in historically climate-limited, infrequent fire regimes for which empirical fire data are lacking. Our analysis and approach address these challenges, demonstrating that spatial scaling relationships (i.e., relationships between fire size and expected patterns of burn severity) offer a means to anticipate future fire effects at a regional scale. The approach we present here can be used to evaluate the potential outcomes of different area burned and fire-size distribution scenarios, with our case study illustrating how the ecological effects of a given total burned area might vary depending on how it is distributed in terms of the number and size of individual fire events (i.e., a small number of very large fires vs. many smaller fires). Our results suggest a given total area that is burned in a few large fires will result in larger high-severity patches with interior areas farther from unburned seed sources, as compared with the same total area being burned in more numerous but smaller fire events. Studies such as these can prove useful in scenario planning and developing regional prefire and postfire management plans in the face of uncertainty. Furthermore, as projections for total area burned and fire-size distributions continue to be refined, our approach can also be used to put quantitative bounds on more realistic potential outcomes of future fire activity, and therefore management considerations such as postfire planting needs. Overall, these findings have important implications for forest resilience and management in a period of increasing fire activity and shifting fire-size distributions.

AUTHOR CONTRIBUTIONS

Michele S. Buonanduci and Brian J. Harvey conceived and designed the study, with input from all authors. Michele S. Buonanduci led data analysis with input from all authors. Michele S. Buonanduci wrote the first draft of the manuscript, and all authors contributed critically to the drafts and approved the final manuscript.

ACKNOWLEDGMENTS

This research was funded by a U.S. Geological Survey Northwest Climate Adaptation Science Center award G17AC000218 to Michele S. Buonanduci and a Graduate Research Innovation award (No. 21-1-01-26) from the Joint Fire Science Program. Brian J. Harvey acknowledges support from the Jack Corkery and George Corkery Jr. Endowed Professorship in Forest Sciences. We thank two anonymous reviewers for their constructive comments on an earlier version of this manuscript. Any opinions, findings, and conclusions or recommendations expressed in this material are those of the authors and do not necessarily reflect the views of the funding or affiliate organizations.

CONFLICT OF INTEREST STATEMENT

The authors declare no conflicts of interest.

DATA AVAILABILITY STATEMENT

Data and code associated with this research (Buonanduci et al., 2024) are available from Zenodo: https://doi.org/10.5281/zenodo.10974153.

ORCID

Michele S. Buonanduci https://orcid.org/0000-0003-3646-9954
Daniel C. Donato https://orcid.org/0000-0002-2072-9240
Joshua S. Halofsky https://orcid.org/0000-0003-4120-7457
Maureen C. Kennedy https://orcid.org/0000-0003-4670-3302
Brian J. Harvey https://orcid.org/0000-0002-5902-4862

REFERENCES

Abatzoglou, J. T., D. S. Battisti, A. P. Williams, W. D. Hansen, B. J. Harvey, and C. A. Kolden. 2021. "Projected Increases in Western US Forest Fire despite Growing Fuel Constraints." *Communications Earth & Environment* 2: 227.

Agee, J. K. 1993. *Fire Ecology of Pacific Northwest Forests*. Washington, DC: Island Press.

Agee, J. K. 1998. "The Landscape Ecology of Western Forest Fire Regimes." *Northwest Science* 72: 24–34.

Baker, W. L. 2009. *Fire Ecology in Rocky Mountain Landscapes*. Washington, DC: Island Press.

Braziunas, K. H., N. G. Kiel, and M. G. Turner. 2023. "Less Fuel for the Next Fire? Short-Interval Fire Delays Forest Recovery and Interacting Drivers Amplify Effects." *Ecology* 104: e4042.

Buonanduci, M. S., D. C. Donato, J. S. Halofsky, M. C. Kennedy, and B. J. Harvey. 2023. "Consistent Spatial Scaling of High-Severity Wildfire Can Inform Expected Future Patterns of Burn Severity." *Ecology Letters* 26: 1687–99.

Buonanduci, M. S., D. C. Donato, J. S. Halofsky, M. C. Kennedy, and B. J. Harvey. 2024. "Release of Data and Code for Buonanduci et al. 2024 Ecosphere." Zenodo. https://doi.org/10.5281/zenodo.10974154.

Cade, B. S., and B. R. Noon. 2003. "A Gentle Introduction to Quantile Regression for Ecologists." *Frontiers in Ecology and the Environment* 1: 412–420.

Cansler, C. A., and D. McKenzie. 2014. "Climate, Fire Size, and Biophysical Setting Control Fire Severity and Spatial Pattern in the Northern Cascade Range, USA." *Ecological Applications* 24: 1037–56.

Collins, B. M., J. T. Stevens, J. D. Miller, S. L. Stephens, P. M. Brown, and M. P. North. 2017. "Alternative Characterization of Forest Fire Regimes: Incorporating Spatial Patterns." *Landscape Ecology* 32: 1543–52.

Collins, L., R. A. Bradstock, H. Clarke, M. F. Clarke, R. H. Nolan, and T. D. Penman. 2021. "The 2019/2020 Mega-Fires Exposed Australian Ecosystems to an Unprecedented Extent of High-Severity Fire." *Environmental Research Letters* 16: 044029.

Commission for Environmental Cooperation. 1997. "Ecological Regions of North America: Toward a Common Perspective." http://www.cec.org/publications/ecological-regions-of-north-america/.

Coop, J. D., S. A. Parks, C. S. Stevens-Rumann, S. D. Crausbay, P. E. Higuera, M. D. Hurteau, A. Tepley, et al. 2020. "Wildfire-Driven Forest Conversion in Western North American Landscapes." *BioScience* 70: 659–673.

Coop, J. D., S. A. Parks, C. S. Stevens-Rumann, S. M. Ritter, C. M. Hoffman, and J. M. Varner. 2022. "Extreme Fire Spread Events and Area Burned under Recent and Future Climate in the Western USA." *Global Ecology and Biogeography* 31: 1949–59.

Cova, G., V. R. Kane, S. Prichard, M. North, and C. A. Cansler. 2023. "The Outsized Role of California's Largest Wildfires in Changing Forest Burn Patterns and Coarsening Ecosystem Scale." *Forest Ecology and Management* 528: 120620.

Dalton, M. M., P. Mote, and A. K. Snover. 2013. *Climate Change in the Northwest: Implications for Our Landscapes, Waters, and Communities*. Washington, DC: Island Press.

Davis, K. T., M. D. Robles, K. B. Kemp, P. E. Higuera, T. Chapman, K. L. Metlen, J. L. Peeler, et al. 2023. "Reduced Fire Severity Offers Near-Term Buffer to Climate-Driven Declines in Conifer Resilience across the Western United States." *Proceedings of the National Academy of Sciences of the United States of America* 120: e2208120120.

Devroye, L. 1986. *Non-Uniform Random Variate Generation*. New York: Springer.

Donato, D. C., J. B. Fontaine, J. L. Campbell, W. D. Robinson, J. B. Kauffman, and B. E. Law. 2009. "Conifer Regeneration in Stand-Replacement Portions of a Large Mixed-Severity Wildfire in the Klamath–Siskiyou Mountains." *Canadian Journal of Forest Research* 39: 823–838.

Donato, D. C., J. S. Halofsky, and M. J. Reilly. 2020. "Corralling a Black Swan: Natural Range of Variation in a Forest Landscape Driven by Rare, Extreme Events." *Ecological Applications* 30: e02013.

Duane, A., M. Castellnou, and L. Brotons. 2021. "Towards a Comprehensive Look at Global Drivers of Novel Extreme Wildfire Events." *Climatic Change* 165: 43.

Francis, E. J., P. Pourmohammadi, Z. L. Steel, B. M. Collins, and M. D. Hurteau. 2023. "Proportion of Forest Area Burned at High-Severity Increases with Increasing Forest Cover and Connectivity in Western US Watersheds." *Landscape Ecology* 38: 2501–18.

Gill, N. S., M. G. Turner, C. D. Brown, S. I. Glassman, S. L. Haire, W. D. Hansen, E. R. Pansing, S. B. St Clair, and D. F. Tomback. 2022. "Limitations to Propagule Dispersal Will Constrain Postfire Recovery of Plants and Fungi in Western Coniferous Forests." *BioScience* 72: 347–364.

Greene, D. F., and E. A. Johnson. 1989. "A Model of Wind Dispersal of Winged or Plumed Seeds." *Ecology* 70: 339–347.

Hagmann, R. K., P. F. Hessburg, S. J. Prichard, N. A. Povak, P. M. Brown, P. Z. Fulé, R. E. Keane, et al. 2021. "Evidence for Widespread Changes in the Structure, Composition, and Fire Regimes of Western North American Forests." *Ecological Applications* 31: e02431.

Halofsky, J. E., D. L. Peterson, and B. J. Harvey. 2020. "Changing Wildfire, Changing Forests: The Effects of Climate Change on

Fire Regimes and Vegetation in the Pacific Northwest, USA." *Fire Ecology* 16: 4.

Halofsky, J. S., D. R. Conklin, D. C. Donato, J. E. Halofsky, and J. B. Kim. 2018a. "Climate Change, Wildfire, and Vegetation Shifts in a High-Inertia Forest Landscape: Western Washington, U.S.A." *PLoS One* 13: e0209490.

Halofsky, J. S., D. C. Donato, J. F. Franklin, J. E. Halofsky, D. L. Peterson, and B. J. Harvey. 2018b. "The Nature of the Beast: Examining Climate Adaptation Options in Forests with Stand-Replacing Fire Regimes." *Ecosphere* 9: e02140.

Hantson, S., S. Pueyo, and E. Chuvieco. 2016. "Global Fire Size Distribution: From Power Law to Log-Normal." *International Journal of Wildland Fire* 25: 403.

Harvey, B. J., M. S. Buonanduci, and M. G. Turner. 2023. "Spatial Interactions among Short-Interval Fires Reshape Forest Landscapes." *Global Ecology and Biogeography* 32: 586–602.

Harvey, B. J., D. C. Donato, and M. G. Turner. 2016a. "High and Dry: Post-Fire Tree Seedling Establishment in Subalpine Forests Decreases with Post-Fire Drought and Large Stand-Replacing Burn Patches: Drought and Post-Fire Tree Seedlings." *Global Ecology and Biogeography* 25: 655–669.

Harvey, B. J., D. C. Donato, and M. G. Turner. 2016b. "Drivers and Trends in Landscape Patterns of Stand-Replacing Fire in Forests of the US Northern Rocky Mountains (1984–2010)." *Landscape Ecology* 31: 2367–83.

Hemstrom, M. A., and J. F. Franklin. 1982. "Fire and Other Disturbances of the Forests in Mount Rainier National Park." *Quaternary Research* 18: 32–51.

Hijmans, R. J., J. van Etten, M. Sumner, J. Cheng, D. Baston, A. Bevan, R. Bivand, et al. 2022. "Package 'raster'." https://CRAN.R-project.org/package=raster.

Hood, S. M., B. J. Harvey, P. J. Fornwalt, C. E. Naficy, W. D. Hansen, K. T. Davis, M. A. Battaglia, C. S. Stevens-Rumann, and V. A. Saab. 2021. "Fire Ecology of Rocky Mountain Forests." In *Fire Ecology and Management: Past, Present, and Future of US Forested Ecosystems*, edited by C. H. Greenberg and B. Collins, 287–336. Cham: Springer International Publishing.

Johnston, J. D., M. R. Schmidt, A. G. Merschel, W. M. Downing, M. R. Coughlan, and D. G. Lewis. 2023. "Exceptional Variability in Historical Fire Regimes across a Western Cascades Landscape, Oregon, USA." *Ecosphere* 14: e4735.

Juang, C. S., A. P. Williams, J. T. Abatzoglou, J. K. Balch, M. D. Hurteau, and M. A. Moritz. 2022. "Rapid Growth of Large Forest Fires Drives the Exponential Response of Annual Forest-Fire Area to Aridity in the Western United States." *Geophysical Research Letters* 49: e2021GL097131.

Kemp, K. B., P. E. Higuera, and P. Morgan. 2016. "Fire Legacies Impact Conifer Regeneration across Environmental Gradients in the U.S. Northern Rockies." *Landscape Ecology* 31: 619–636.

Kennedy, M. C. 2019. "Experimental Design Principles to Choose the Number of Monte Carlo Replicates for Stochastic Ecological Models." *Ecological Modelling* 394: 11–17.

Kennedy, M. C., R. R. Bart, C. L. Tague, and J. S. Choate. 2021. "Does Hot and Dry Equal More Wildfire? Contrasting Short- and Long-Term Climate Effects on Fire in the Sierra Nevada, CA." *Ecosphere* 12(7): e03657.

Koenker, R., and G. Bassett. 1978. "Regression Quantiles." *Econometrica* 46: 33.

Laughlin, M. M. 2023. "Patterns and Drivers of Early Conifer Regeneration Following Stand-Replacing Wildfire in Pacific Northwest (USA) Temperate Maritime Forests." *Forest Ecology and Management* 549: 121491.

LeCompte-Mastenbrook, J. K. 2015. "Restoring Coast Salish Foods and Landscapes: A More-than-Human Politics of Place, History and Becoming." Dissertation, University of Washington.

Littell, J. S., D. McKenzie, H. Y. Wan, and S. A. Cushman. 2018. "Climate Change and Future Wildfire in the Western United States: An Ecological Approach to Nonstationarity." *Earth's Future* 6: 1097–1111.

Littlefield, C. E. 2019. "Topography and Post-Fire Climatic Conditions Shape Spatio-Temporal Patterns of Conifer Establishment and Growth." *Fire Ecology* 15: 34.

Long, J. W., F. K. Lake, and R. W. Goode. 2021. "The Importance of Indigenous Cultural Burning in Forested Regions of the Pacific West, USA." *Forest Ecology and Management* 500: 119597.

Lydersen, J. M., B. M. Collins, J. D. Miller, D. L. Fry, and S. L. Stephens. 2016. "Relating Fire-Caused Change in Forest Structure to Remotely Sensed Estimates of Fire Severity." *Fire Ecology* 12: 99–116.

Malamud, B. D., J. D. A. Millington, and G. L. W. Perry. 2005. "Characterizing Wildfire Regimes in the United States." *Proceedings of the National Academy of Sciences of the United States of America* 102: 4694–99.

Mauger, G., J. H. Casola, H. A. Morgan, R. L. Strauch, B. Jones, B. Curry, T. M. Busch Isaksen, L. Whitely Binder, M. B. Krosby, and A. K. Snover. 2015. "State of Knowledge: Climate Change in Puget Sound." Report Prepared for the Puget Sound Partnership and the National Oceanic and Atmospheric Administration, Climate Impacts Group, University of Washington, Seattle.

McColl-Gausden, S. C., L. T. Bennett, H. G. Clarke, D. A. Ababei, and T. D. Penman. 2022. "The Fuel–Climate–Fire Conundrum: How Will Fire Regimes Change in Temperate Eucalypt Forests under Climate Change?" *Global Change Biology* 28: 5211–26.

McKenzie, D., and M. C. Kennedy. 2011. "Scaling Laws and Complexity in Fire Regimes." In *The Landscape Ecology of Fire*, edited by D. McKenzie, C. Miller, and D. A. Falk, 27–49. Dordrecht: Springer Netherlands.

Miller, J. D., and A. E. Thode. 2007. "Quantifying Burn Severity in a Heterogeneous Landscape with a Relative Version of the Delta Normalized Burn Ratio (dNBR)." *Remote Sensing of Environment* 109: 66–80.

Muggeo, V. M. R. 2021. "Additive Quantile Regression with Automatic Smoothness Selection: The R Package QuantregGrowth." https://CRAN.R-project.org/package=quantregGrowth.

Neel, M. C., K. McGarigal, and S. A. Cushman. 2004. "Behavior of Class-Level Landscape Metrics across Gradients of Class Aggregation and Area." *Landscape Ecology* 19: 435–455.

Newman, E. A., M. C. Kennedy, D. A. Falk, and D. McKenzie. 2019. "Scaling and Complexity in Landscape Ecology." *Frontiers in Ecology and Evolution* 7: 293.

Parks, S. A., and J. T. Abatzoglou. 2020. "Warmer and Drier Fire Seasons Contribute to Increases in Area Burned at High Severity in Western US Forests from 1985 to 2017." *Geophysical Research Letters* 47(22): e2020GL089858.

Parks, S. A., L. M. Holsinger, M. H. Panunto, W. M. Jolly, S. Z. Dobrowski, and G. K. Dillon. 2018a. "High-Severity Fire: Evaluating Its Key Drivers and Mapping Its Probability across Western US Forests." *Environmental Research Letters* 13: 044037.

Parks, S. A., L. Holsinger, M. Voss, R. Loehman, and N. Robinson. 2018b. "Mean Composite Fire Severity Metrics Computed with Google Earth Engine Offer Improved Accuracy and Expanded Mapping Potential." *Remote Sensing* 10: 879.

Pebesma, E. 2018. "Simple Features for R: Standardized Support for Spatial Vector Data." *The R Journal* 10: 439.

Prichard, S. J., P. F. Hessburg, R. K. Hagmann, N. A. Povak, S. Z. Dobrowski, M. D. Hurteau, V. R. Kane, et al. 2021. "Adapting Western North American Forests to Climate Change and Wildfires: 10 Common Questions." *Ecological Applications* 31: e02433.

Prichard, S. J., N. A. Povak, M. C. Kennedy, and D. W. Peterson. 2020. "Fuel Treatment Effectiveness in the Context of Landform, Vegetation, and Large, Wind-Driven Wildfires." *Ecological Applications* 30: e02104.

Pueyo, S. 2014. "Algorithm for the Maximum Likelihood Estimation of the Parameters of the Truncated Normal and Lognormal Distributions." arXiv.

Reilly, M. J., C. J. Dunn, G. W. Meigs, T. A. Spies, R. E. Kennedy, J. D. Bailey, and K. Briggs. 2017. "Contemporary Patterns of Fire Extent and Severity in Forests of the Pacific Northwest, USA (1985-2010)." *Ecosphere* 8: e01695.

Reilly, M. J., J. E. Halofsky, M. A. Krawchuk, D. C. Donato, P. F. Hessburg, J. D. Johnston, A. G. Merschel, M. E. Swanson, J. S. Halofsky, and T. A. Spies. 2021. "Fire Ecology and Management in Pacific Northwest Forests." In *Fire Ecology and Management: Past, Present, and Future of US Forested Ecosystems*, edited by C. H. Greenberg and B. Collins, 393–435. Cham: Springer International Publishing.

Reilly, M. J., A. Zuspan, J. S. Halofsky, C. Raymond, A. McEvoy, A. W. Dye, D. C. Donato, et al. 2022. "Cascadia Burning: The Historic, but Not Historically Unprecedented, 2020 Wildfires in the Pacific Northwest, USA." *Ecosphere* 13(6): e4070.

Rollins, M. G. 2009. "LANDFIRE: A Nationally Consistent Vegetation, Wildland Fire, and Fuel Assessment." *International Journal of Wildland Fire* 18: 235.

Romme, W. H., M. S. Boyce, R. Gresswell, E. H. Merrill, G. W. Minshall, C. Whitlock, and M. G. Turner. 2011. "Twenty Years after the 1988 Yellowstone Fires: Lessons about Disturbance and Ecosystems." *Ecosystems* 14: 1196–1215.

Saberi, S. J., and B. J. Harvey. 2023. "What Is the Color When Black Is Burned? Quantifying (re)Burn Severity Using Field and Satellite Remote Sensing Indices." *Fire Ecology* 19: 24.

Singleton, M. P., A. E. Thode, A. J. Sánchez Meador, and J. M. Iniguez. 2019. "Increasing Trends in High-Severity Fire in the Southwestern USA from 1984 to 2015." *Forest Ecology and Management* 433: 709–719.

Spies, T. A., P. A. Stine, R. A. Gravenmier, J. W. Long, and M. J. Reilly. 2018. *Synthesis of Science to Inform Land Management within the Northwest Forest Plan Area*. PNW-GTR-966. Portland, OR: U.S. Department of Agriculture, Forest Service, Pacific Northwest Research Station.

Steel, Z. L., A. M. Fogg, R. Burnett, L. J. Roberts, and H. D. Safford. 2022. "When Bigger Isn't Better—Implications of Large High-Severity Wildfire Patches for Avian Diversity and Community Composition." *Diversity and Distributions* 28: 439–453.

Stevens, J. T., B. M. Collins, J. D. Miller, M. P. North, and S. L. Stephens. 2017. "Changing Spatial Patterns of Stand-Replacing Fire in California Conifer Forests." *Forest Ecology and Management* 406: 28–36.

Swanson, M. E., J. F. Franklin, R. L. Beschta, C. M. Crisafulli, D. A. DellaSala, R. L. Hutto, D. B. Lindenmayer, and F. J. Swanson. 2011. "The Forgotten Stage of Forest Succession: Early-Successional Ecosystems on Forest Sites." *Frontiers in Ecology and the Environment* 9: 117–125.

Tepley, A. J., F. J. Swanson, and T. A. Spies. 2013. "Fire-Mediated Pathways of Stand Development in Douglas-Fir/Western Hemlock Forests of the Pacific Northwest, USA." *Ecology* 94: 1729–43.

Turner, M. G., K. H. Braziunas, W. D. Hansen, and B. J. Harvey. 2019. "Short-Interval Severe Fire Erodes the Resilience of Subalpine Lodgepole Pine Forests." *Proceedings of the National Academy of Sciences of the United States of America* 116: 11319–28.

Wang, X., K. Studens, M.-A. Parisien, S. W. Taylor, J.-N. Candau, Y. Boulanger, and M. D. Flannigan. 2020. "Projected Changes in Fire Size from Daily Spread Potential in Canada over the 21st Century." *Environmental Research Letters* 15: 104048.

Waring, R. H., and J. F. Franklin. 1979. "Evergreen Coniferous Forests of the Pacific Northwest." *Science* 204: 1380–86.

Westerling, A. L., M. G. Turner, E. A. H. Smithwick, W. H. Romme, and M. G. Ryan. 2011. "Continued Warming Could Transform Greater Yellowstone Fire Regimes by Mid-21st Century." *Proceedings of the National Academy of Sciences of the United States of America* 108: 13165–70.

Wood, S. 2022. "Package 'mgcv'."

Wynecoop, M. D., P. Morgan, E. K. Strand, and F. Sanchez Trigueros. 2019. "Getting Back to Fire sumés: Exploring a Multi-Disciplinary Approach to Incorporating Traditional Knowledge into Fuels Treatments." *Fire Ecology* 15: 17.

SUPPORTING INFORMATION

Additional supporting information can be found online in the Supporting Information section at the end of this article.

How to cite this article: Buonanduci, Michele S., Daniel C. Donato, Joshua S. Halofsky, Maureen C. Kennedy, and Brian J. Harvey. 2024. "Few Large or Many Small Fires: Using Spatial Scaling of Severe Fire to Quantify Effects of Fire-Size Distribution Shifts." *Ecosphere* 15(6): e4875. https://doi.org/10.1002/ecs2.4875